Separation and Purification Technology 354 (2025) 128969

Contents lists available at ScienceDirect

Separation and Purification Technology

journal homepage: www.elsevier.com/locate/seppur

One-step purification of L-asparaginase from cell extracts using carbon xerogels

Raquel O. Cristóvão [a,b], Rita A.M. Barros [a,b], Teresa P. Marramaque [a,b], Gonçalo G. Aguiar [a,b], Mafalda R. Almeida [c], Sónia A.C. Carabineiro [a,d], Gabriela B. de Paiva [e], Danielle B. Pedrolli [e], Mara G. Freire [c], Joaquim L. Faria [a,b], Valéria C. Santos-Ebinuma [e], Ana P.M. Tavares [c,*], Cláudia G. Silva [a,b,*]

[a] LSRE-LCM - Laboratory of Separation and Reaction Engineering – Laboratory of Catalysis and Materials, Faculty of Engineering, University of Porto, Rua Dr. Roberto Frias, 4200-465 Porto, Portugal
[b] ALiCE – Associate Laboratory in Chemical Engineering, Faculty of Engineering, University of Porto, Rua Dr. Roberto Frias, 4200-465 Porto, Portugal
[c] CICECO-Aveiro Institute of Materials, Department of Chemistry, University of Aveiro, 3810-193 Aveiro, Portugal
[d] LAQV-REQUIMTE, Department of Chemistry, NOVA School of Science and Technology, Universidade NOVA de Lisboa, 2829-516 Caparica, Portugal
[e] Department of Bioprocess Engineering and Biotechnology, School of Pharmaceutical Sciences, UNESP-University Estadual Paulista, Araraquara, Brazil

ARTICLE INFO

Keywords:
Aliivibrio fischeri L-asparaginase
Purification
Carbon xerogels
Adsorbent materials
Flow-through-like mode
Cell extract

ABSTRACT

L-asparaginase (ASNase, EC 3.5.1.1) is an enzyme with wide applications in the pharmaceutical sector and food processing industries. It is mainly used as a biotherapeutic for treating Acute Lymphoblastic Leukemia (ALL) and to reduce acrylamide formation in starchy compounds. Despite its relevance, current purification methods for microbial enzymes involve complex and expensive techniques. To overcome this drawback, Carbon Xerogels (CXs) were here investigated as novel adsorbents to be applied in an one-step ASNase purification process, using a flow-through-like setup, from a cell extract of genetically engineered *Bacillus subtilis*. Different operating conditions were studied for optimizing the adsorption onto CXs, including total protein concentration (3–15 mg/mL), CXs amount (12, 18 and 24 mg), and adsorption volume of cell extract (1.5, 2.0 and 15 mL). Ultimately, CXs were packed into a column to evaluate the feasibility of semi-continuous ASNase purification. CXs have high affinity for other proteins present in the cell extract, while leaving ASNase in the supernatant or eluted sample. Purification folds of 2.5 and 3.8 for ASNase were obtained in batch and semi-continuous experiments, respectively, revealing the potential of CXs as novel adsorbent materials for ASNase purification directly from a complex matrix.

1. Introduction

Proteins, particularly enzymes, show extensive applications in diverse industrial fields. Among these, L-asparaginase (L-asparagine amidohydrolase, EC 3.5.1.1 – ASNase) is an enzyme that has been showing significant progress in the worldwide biocatalyst market over the past two decades [1]. Its mechanism of action focuses on catalyzing the hydrolysis of the amino acid L-asparagine (L-asn) into L-aspartic acid and ammonium [2]. Two types of ASNase are reported in the literature: type I, characterized by low affinity for L-asparagine and high affinity for L-glutamine, and type II, recognized by its high L-asparagine affinity and low L-glutamine affinity [3]. Therefore, ASNase type I has been used in the mitigation of toxic acrylamide production in high-temperature processed foods, while ASNase type II has been employed to deprive cancer cells of L-asparagine, essential for their growth, making this enzyme a highly sought-after in both food and medical fields.

ASNase can be produced by a wide variety of microorganisms, including bacteria and fungi, algae, plants, and some animals. The biopharmaceutical version is typically produced by genetically modified microorganisms [3]. After production, attention must be given to the costly downstream processing stage, particularly the purification process. The enzyme purification steps directly influence the market price of the product, with downstream processing accounting for up to 80 % of the total cost [4]. The main requirement of any purification method of biomolecules is to maximize product recovery, while assuring their high purity, without compromising their biological activity [5]. Current

* Corresponding authors.
E-mail addresses: aptavares@ua.pt (A.P.M. Tavares), cgsilva@fe.up.pt (C.G. Silva).

https://doi.org/10.1016/j.seppur.2024.128969
Received 3 June 2024; Received in revised form 23 July 2024; Accepted 24 July 2024
Available online 26 July 2024

enzyme purification processes are mainly focused on chromatographic techniques, membranes, precipitation methods, and liquid–liquid or solid–liquid extractions. In most cases, a sequential combination of purification techniques is needed to achieve the desired purity, making the process expensive, time-consuming, and laborious [6,7]. Consequently, these factors have a negative impact on the final cost of the biomolecule [8,9].

The ASNase purification usually resorts to methods such as ammonium sulfate precipitation [10,11], followed by chromatography techniques, such as affinity chromatography [12,13], ion exchange [14,15] and size exclusion chromatography [16,17], ultrafiltration [18,19], among others. Due to its accuracy, scalability, robustness, selectivity, and reliability, chromatography is frequently used in most ASNase purification processes [8]. However, chromatographic methods have shown some drawbacks, like long processing times, high costs of the resins employed, and low yields [20].

To overcome these limitations, there is a high demand for efficient, simple, and economically feasible alternatives to purify ASNase.

Carbon-based nanomaterials have been successfully used as supports for protein adsorption due to their unique structure, pore size, high surface area, and adsorption capacity [21,22]. In particular, carbon xerogels (CXs), with tunable porosity through changes in the synthesis conditions, are highly attractive support materials for ASNase attachment when foreseeing catalytic applications [23–25].

This work aims to investigate CXs for the one-step ASNase purification directly from a cell extract of genetically engineered *Bacillus subtilis*. The first phase involved the synthesis and characterization of CXs, followed by evaluation of the ASNase purification through the adsorption of other proteins on the material (flow-through-like mode), using both batch and semi-continuous processes. Several parameters, such as cell extract concentration, nanomaterial mass, and adsorption volume, were optimized for maximizing ASNase purification. Finally, the potential for CXs reuse was investigated by assessing the desorption of the non-target proteins from the support by variations in pH, temperature, and salt concentration.

2. Experimental section

2.1. Chemicals

Lyophilized (without additives) and purified type II ASNase from *E. coli* (P1321-10000; 10,000 IU) were supplied by Deltaclon S.L., Spain. L-asn (≥99.0 %). Tris(hydroxymethyl)aminomethane (TRIS) (≥99.0 %), disodium hydrogen phosphate (≥99.0 %) and phosphate buffered saline (PBS) tablets were purchased from VWR International, LLC. Trichloroacetic acid (TCA) (≥99.0 %) was obtained from J.T. Baker. Citric acid (≥99.5 %) and Nessler's reagent (dipotassium tetraiodomercurate (II)) was supplied by Merck Chemical Company (Germany). Sodium hydroxide (≥98.0 %) and hydrochloric acid (37 %) were bought from Sigma-Aldrich. Bovine serum albumin (BSA) was supplied by Acros Organic, PA.

2.2. ASNase cell extract

The ASNase cell extract from *Aliivibrio fischeri* was obtained according to a procedure described elsewhere [26]. Briefly, an inoculum was prepared by the activation of a stock culture of engineered *B. subtilis* (20 % v/v in glycerol maintained at −80 °C) in 15 mL of *Luria Bertani* (LB) medium supplemented with erythromycin (1 μg/mL) in 50 mL Falcon tubes. The cells were grown at 37 °C, overnight (14–16 h) in an orbital shaker. The ASNase production was initiated by transferring the *B. subtilis* inoculum culture to 1 L Erlenmeyer flasks containing 250 mL of medium. The initial optical density at 600 nm ($OD_{600\ nm}$) was adjusted to 0.1 absorbance units (AU) using a spectrophotometer. The bioprocess was carried out at 37 °C and 220 rpm. When the $OD_{600\ nm}$ reached between 0.7 and 1 AU, 0.5 % w/v xylose was added to induce ASNase production. The bioprocess continued for 24 h at 30 °C and 220 rpm. The cells were then harvested by centrifugation (12000 × G, 4 °C, 10 min). The resulting pellets were resuspended in 10 mL PBS buffer. Ultrasound sonication was used to recover the intracellular ASNase, resulting in a cell extract with an initial total protein concentration of 24 mg/mL. The reported ASNase isoelectric point (*pI*) is between 5.0 and 5.7 [27].

2.3. Synthesis of CXs

The CXs were synthesized according to a previously described method [28,29]. The materials were obtained through a polycondensation reaction between resorcinol and formaldehyde in aqueous media, with a molar ratio of 1:2. The pH of the solution was adjusted to 6.0 using 5 M NaOH to obtain CXs with an average pore diameter of 12 nm. The solution was then heated in an oil bath at 65 °C, with a temperature increase of 5 °C every 15 min up to 85 °C, maintained constant for 3 days. The resulting solid, opaque gel, was ground into granules measuring approximately 0.5–1 cm in diameter. The solvent was removed by drying the material in a muffle furnace for one week, with the temperature gradually increased from 60 and 150 °C, at a rate of 20 °C per day. The material was then pyrolyzed at 800 °C in N_2, with a flow rate of 100 mL/min, with an oven heating in 3 steps: 1 °C/min from room temperature to 150 °C, maintained for 15 min; 5 °C/min until 400 °C, maintained for 60 min; 5 °C/min until 800 °C, maintained for 120 min. Finally, the resulting material was ground, sieved, and the desired particle size granulometry (between 100 and 500 μm) was selected.

2.4. Characterization of CXs

The textural properties of CXs were analyzed by N_2 adsorption–desorption at –196 °C using a Quantachrome NOVA 4200e apparatus. The Brunauner-Emmett-Teller (BET) specific surface area (S_{BET}) was calculated from nitrogen adsorption in the relative pressure range from 0.05 to 0.15. The Barrett-Joyner-Halenda (BJH) method was applied to the desorption branch to obtain the pore size distribution curve and cumulative volume of pores (V_p).

The Raman spectrum was recorded on a WITec alpha300 R-Confocal Raman Imaging instrument equipped with a laser, operating at an excitation wavelength of 532 nm and a power of 5 mW.

Particle size distribution was determined by laser diffraction using a Malvern Mastersizer 3000 analyzer equipped with a Hydro MV dispersion unit (Malvern, UK), with distilled water as the sample dispersion medium. Five measurements were performed to ensure reproducibility. The results were expressed in volume for 10, 50 and 90 % of the total volume of the particles in the sample. All residual values were less than 1 %.

The morphology of the material was analyzed by scanning electron microscopy (SEM) using a Desktop SEM Phenom ProX microscope operated at an accelerating voltage of 15 kV. Samples for microscopic analysis were prepared by placing the material, after drying at 40 °C, on a glass slide. A thin film of carbon was deposited immediately prior to sample analysis to ensure conductivity.

2.5. Total protein quantification

The total protein concentration of the cell extract was determined by measuring the absorbance at 280 nm (JASCO V-560 UV–Vis spectrophotometer) [30] before and after the adsorption onto CXs, using a calibration curve established with BSA (standard protein).

2.6. ASNase activity quantification

The experimental procedure to quantify the ASNase activity involves the addition of 375 μL of ASNase cell extract, supernatant, or a certain

mass of CXs after adsorption, which was mixed with 500 μL of Tris-HCl buffer (pH 8.6, 50 mM), 50 μL of 189 mM L-asn solution in PBS buffer, and 125 μL of distilled water. Mixtures were incubated for 30 min at 37 °C under stirring. After incubation, the enzymatic reaction was stopped by adding 250 μL of TCA (1.5 M) in the fume hood. Due to the high protein concentration, a centrifugation step at 136 G for 5 min was performed, after the addition of TCA, to separate precipitated proteins from the supernatant. The amount of ammonium released after the hydrolysis of L-asn was measured by adding 375 μL of supernatant of each sample to 250 μL of Nessler's reagent and 625 μL of distilled water. A control sample containing 1 mL of water and 250 μL of Nessler reagent was used. After 30 min of incubation at room temperature, the absorbance was measured at 436 nm (using a JASCO V-560 UV–Vis spectrophotometer). The activity of the ASNase was calculated by Eq. (1), where one unit of ASNase activity (U) corresponds to the amount of enzyme that releases 1 μmol of ammonium per minute:

$$ASNase\ activity\left(\frac{U}{mL}\right) = \frac{\left[NH_4^+\right]\left(\frac{\mu mol}{mL}\right) \times V_{Nessler}(mL) \times f_d}{V_{Enzyme}(mL) \times t_r(min)} \quad (1)$$

where $V_{Nessler}$ is the volume of the Nessler solution, f_d is the sample dilution factor, V_{Enzyme} is the volume of the cell extract, and t_r is the reaction time.

The activity of ASNase adsorbed onto CXs was determined using Eq. (2):

$$ASNase\ activity\left(\frac{U}{mg}\right) = \frac{\left[NH_4^+\right]\left(\frac{\mu mol}{L}\right) \times V_{Nessler}(L) \times f_d}{t_r(min) \times m_s(mg)} \quad (2)$$

where m_s is the mass (mg) of the support.

With the total protein and ASNase activity obtained before and after adsorption, the ASNase specific activity was calculated using Eq. (3):

$$ASNase\ specific\ activity\left(\frac{U}{mg}\right) = \frac{ASNase\ enzymatic\ activity\left(\frac{U}{mL}\right)}{Total\ protein\left(\frac{mg}{mL}\right)} \quad (3)$$

The ASNase purification fold in the supernatant was determined using Eq. (4):

$$Purification\ fold = \frac{ASNase\ specific\ activity_{after\ \ adsorption}\left(\frac{U}{mg}\right)}{ASNase\ specific\ activity_{extract}\left(\frac{U}{mg}\right)} \quad (4)$$

2.7. Protein profile by SDS-PAGE

The protein profile of the supernatants was evaluated by sodium dodecyl sulphate–polyacrylamide gel electrophoresis (SDS-PAGE). Samples were diluted at a 1:1 (v/v) ratio in a sample buffer composed of 2.5 mL of 0.5 M Tris-HCl pH 6.8, 4.0 mL of 10 % (m/v) SDS solution, 2 mg of bromophenol blue, 2.0 mL of glycerol and 310 mg of dithiothreitol (DTT). After this dilution, samples were heated at 95 °C, for 5 min. The diluted samples were loaded and run on a polyacrylamide gel (stacking: 4 % and resolving: 20 %). To stain the proteins, the gels were impregnated with BlueSafe and stirred in an orbital shaker at 50 rpm, overnight at room temperature. Amersham™ ECL™ Rainbow™ Marker – Full range was used as molecular weight standards, while lyophilized and purified ASNase from *E. coli* was used as a pure ASNase standard.

2.8. Batch purification of ASNase from the cell extract

2.8.1. Adsorption of non-target proteins from the cell extract onto CXs

ASNase purification using CXs was studied by adding 1.5 mL of different total protein concentrations (from 3.0 to 15 mg/mL) of the cell extract from *B. subtilis* to 12, 18 and 24 mg of material in 1.5, 2.0 and 15 mL flasks. The ASNase purification was performed by stirring the mixtures for 1 h in a multifunctional tube rotator (Grant Instruments Lda., model PTR-35), followed by samples centrifugation at 136 G for 6 min to separate the material from the supernatant. A control solution containing 375 μL of the initial extract without contact with the material was prepared. All experiments were performed in duplicate.

2.8.2. Protein desorption from CXs

The desorption of the unwanted proteins of the cell extract from the CXs was assessed by 3 different methods: by changing the pH of the solution with a pH 4.0 citrate buffer, by the effect of temperature at 80 °C and by increasing the salt concentration with a 5 mM NaCl solution. The desorption process consisted of adding to the materials 1.5 mL of buffer, NaCl solution or distilled water, respectively, for each of the methods, followed by a 1 h incubation period with controlled temperature. After incubation, the materials were centrifuged at 136 G for 10 min to separate them from the supernatant. The percentage of protein desorption was determined based on the protein concentration in the supernatant.

2.9. Semi-continuous ASNase purification from the cell extract

2.9.1. Adsorption of non-target proteins from the cell extract onto CXs

In the semi-continuous purification process, a YMC Glass Column (ECO 10/120M4V-K) with an internal diameter of 10 mm, a length of 120 mm, and a maximum operating pressure of 30 bar was used (Figure S1). The column was packed with CXs, previously mixed with distilled water and degassed under vacuum in an ultrasonic bath for 2 h, resulting in a bed height of 5 cm. A peristaltic pump (ISMATEC ISM 596 REGLO Digital MS-2/12) operating at a flow rate of 1 mL/min was used to feed the cell extract (3 mg/mL). Samples of 1.5 mL each were withdrawn over a 6 h period, for subsequent analysis of total protein and ASNase activity.

2.9.2. Protein desorption from CXs

Desorption of the proteins from the CXs packed in the column was carried out for 24 h at a flow rate of 1.5 mL/min, using distilled water at 50 °C. Several samples (1.5 mL each) were collected over time for the determination of the total protein concentration.

3. Results and discussion

3.1. CXs characterization

The synthesized CXs were characterized using N_2 adsorption at −196 °C. The BET method revealed a surface area of 688 m^2/g. The BJH method confirmed an average pore radius (r_p) of 6.3 nm, and a total pore volume (V_p) of 0.80 cm^3/g. The pore radius distribution is presented in Figure S2 in the Supporting Information.

To verify whether the sieving process after CXs synthesis effectively restricted the particle size within the desired range, the size distribution was evaluated, as shown in Figure S3 in the Supporting Information. The obtained results show that 10, 50 and 90 % of the total particle volume corresponds to sizes of 130 μm, 252 μm and 387 μm, respectively. The synthesized CXs exhibit an average size of 252 μm, confirming that the sieving process successfully allowed the desired size range. Approximately 95 % of the total particle volume shows a size between 100 and 500 μm.

The CXs morphology was examined using scanning electron microscopy (SEM). Figure S4 shows that the synthesized CXs particles are large, and non-homogeneous structures with an irregular morphology, being in agreement with the results reported by Barros et al. [23].

Raman spectroscopy was also used to characterize the surface of the synthesized CXs. The Raman spectrum, depicted in Figure S5 in the Supporting Information, exhibits two prominent bands in the spectral

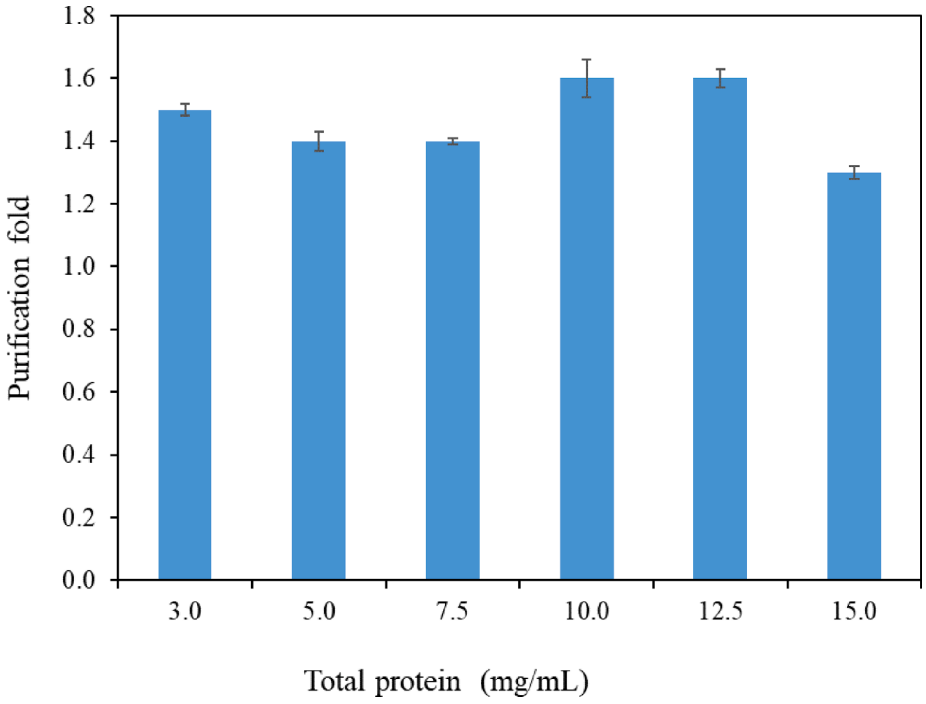

Fig. 1. ASNase purification fold after adsorption of different total protein concentrations of cell extract from *B. subtilis* (from 3 to 15 mg/mL) onto 12 mg CX in 1.5 mL flasks. Error bars represent the standard deviation between replicates.

region between 1000 and 2000 cm^{-1}, characteristic of carbon nanomaterials. The D band peak observed at around 1400 cm^{-1} is associated with point defects and disorder in carbon atoms with sp^3 hybridization. The G-band peaks at approximately 1650 cm^{-1} correspond to bond vibrations of carbon atoms with sp^2 hybridization [31,32].

3.2. Batch purification of ASNase from cell extract

3.2.1. Adsorption of non-target proteins onto CXs

For evaluating the adsorption capacity of CXs towards the proteins present in the cell extract containing ASNase from *B. subtilis*, various total protein concentrations (ranging from 3 to 15 mg/mL) were considered. These were placed in contact with different amounts of CXs. No buffer solution was used for protein adsorption, only the cell extract was used. The first assays were carried out using the optimized adsorption material mass of 2 mg, obtained for the commercial ASNase [23]. However, due to the high total protein concentration in the cell extract, it was noticed that 2 mg of support was insufficient to capture a significant fraction of the proteins in the solution, leading to a fast saturation of the CXs. Therefore, the amount of CXs was increased to 12 mg.

While previous immobilization studies with pure commercial enzyme demonstrated the high affinity of this material for ASNase adsorption, resulting in complete adsorption of ASNase onto the CXs [23], the results obtained with the complex cell extract were different. In the presence of the cell extract, only a small fraction of ASNase was conjugated with the CXs in all the tested conditions, with the remaining proteins from the cell extract being preferentially adsorbed. This was evident from the higher specific ASNase activity observed in the supernatant recovered after contact of the cell extract with CXs.

As reported by Barros et al. [24], untreated CXs lack functional groups on their surface, making them highly hydrophobic materials. On the other hand, it was also demonstrated that varying the solution pH has little or no influence on the ASNase adsorption onto CXs [23]. In fact, taking into account the *pI* of ASNase (between 5.0 and 5.7) and the point of zero charge of CXs (pH_{pzc} = 6.0 [23]), the pH range values in which the enzyme and the support have opposite charges is quite narrow. This suggests that electrostatic interactions are unlikely to be the most important interactions driving enzyme adsorption. This way, it can be assumed that the mechanism of protein binding onto CXs is mainly through hydrophobic interactions, van der Waals forces and π-π stacking interactions.

Table 1
ASNase purification fold after adsorption of 3 mg/mL total protein concentration of cell extract from *B. subtilis* onto different amounts of CXs (12, 18 and 24 mg), in various volume flasks.

CXs mass (mg)	Purification fold		
	1.5 mL tubes	2.0 mL tubes	15 mL tubes
12	1.54 ± 0.02	0.85 ± 0.02	0.66 ± 0.12
18	0.78 ± 0.03	0.92 ± 0.01	1.63 ± 0.03
24	0.69 ± 0.01	1.10 ± 0.01	0.81 ± 0.06

The purification fold was determined by the number of times the specific activity of ASNase increased in the supernatant after the applied purification method. Purification folds varied from 1.3 and 1.6 (Fig. 1), suggesting that other proteins (impurities) had a higher affinity for adsorption onto the material, leaving the ASNase free in the supernatant. However, quantitatively, no trend or clear relationship was observed between the cell extract total protein concentration and the purification fold. Therefore, it was decided to proceed with the cell extract with the lower concentration of proteins, 3 mg/mL, in order to promote the adsorption of impurities onto the CXs and increase the ASNase purity in the supernatant.

To study the effect of the amount of material and adsorption volume on the ASNase purification, different combinations of cell extract concentration, material mass, and adsorption volume were examined. 3 mg/mL of cell extract were adsorbed onto 12, 18 and 24 mg of CX in tube flasks with volumes of 1.5, 2.0 and 15 mL. The obtained results (Table 1) suggest that the most promising combination for ASNase purification is achieved by adsorbing 3 mg/mL of cell extract onto 18 mg of CX in a 15 mL tube flask, resulting in a purification fold of 1.63. However, once again, there was no clear trend in the results obtained.

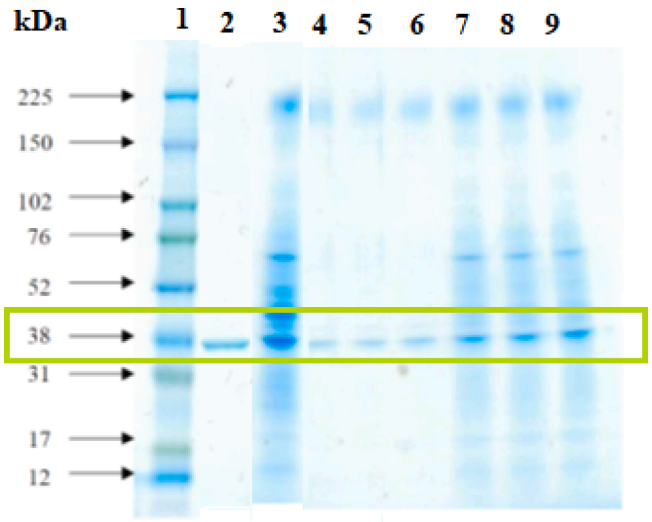

Fig. 2. SDS-PAGE analysis of several samples: Lane 1: Protein marker; Lane 2: Commercial ASNase from *E. coli*; Lane 3: ASNase cell extract from *B. subtilis* 3 mg/mL; Lane 4: ASNase cell extract purified with 12 mg of CXs in 15 mL flasks; Lane 5: ASNase cell extract purified with 18 mg of CXs in 15 mL flasks; Lane 6: ASNase cell extract purified with 24 mg of CXs in 15 mL flasks; Lane 7: ASNase cell extract purified with 12 mg of CXs in 1.5 mL flasks; Lane 8: ASNase cell extract purified with 18 mg of CXs in 1.5 mL flasks; Lane 9: ASNase cell extract purified with 24 mg of CXs in 1.5 mL flasks.

Accordingly, SDS-PAGE was used to examine the protein profile of the cell extracts in the supernatants. This analysis was conducted for the two adsorption volume conditions where the best purification folds were found (1.5 and 15 mL tubes).

Fig. 2 shows the SDS-PAGE results, illustrating the protein profiles of the supernatants relative to the adsorption volume conditions. Lane 2 represents the pure commercial ASNase from *E. coli*, showing a single band (around 38 kDa). On the other hand, lane 3, corresponding to the 3 mg/mL cell extract (lane 3), demonstrates the presence of ASNase (band around 38 kDa) along with several other proteins. From Fig. 2, it can be qualitatively noticed that CXs were able to selectively leave the ASNase in the supernatant, leading to a significant reduction in the number of other proteins, when using 15 mL tubes (lanes 4, 5 and 6) for the ASNase purification. In fact, CXs demonstrate a preference for adsorbing the smaller proteins present in the cell extract, allowing the target ASNase to remain in the supernatant solution, corroborating the results given in Table 1. The most interesting characteristic of CXs is their porous structure and controlled pore size distribution, which can be tailored with relatively high precision. This specific pore size is the main property responsible for the selective isolation of ASNase enzyme from other proteins present in the cell extract. It should be noted that typically, active bacterial type II ASNase are 140–150 kDa tetramers (large proteins) formed by four identical subunits [33]. However, due to the reducing conditions applied to perform the SDS-PAGE analysis, such as the addition of DTT and the heating of the samples, ASNase appears broken down in its monomeric form at 38 kDa in the SDS-PAGE results (Fig. 2). Comparing the pore diameter size of CXs (12 nm) with the size of the ASNase molecule (140 KDa, corresponding to a diameter size of 6.9 nm [34]), it is possible to infer that when using purified ASNase, the CXs are able to adsorb the enzyme, as reported by Barros et al. [24]. However, in the presence of other molecules, CXs have a higher affinity for the smaller proteins, leaving the larger ones, such as ASNase, free in solution. In fact, these results describe an aimed approach, i.e. to purify ASNase by the flow-through-like mode. Preserving the free ASNase in supernatant, without the presence of other proteins and without compromising its activity in desorption steps, is the ideal foreseen cost-effective purification strategy.

To investigate the influence of contact time on the achieved ASNase purification fold, the cell extract was left in contact with 18 mg of CXs in a 15 mL tube flask for a period of 4.5 h. Under these conditions, it was found that CXs were able to adsorb approximately 45 % of the initial total protein, resulting in an increase of the ASNase purification fold to 2.5 in the supernatant. Moreover, no ASNase activity was detected in the material, reinforcing the high capacity of CXs in effectively adsorb other proteins from the cell extract.

Table 2
Comparison of purification methods of intracellularly produced ASNase, including the respective microorganism source and purification fold.

Purification Methods	Microorganism source	Purification fold	Reference
Ammonium sulphate precipitation + dialysis + ion exchange chromatography	*Streptomyces* sp. NEAE-82	3.3	[36]
Filtration + Ammonium sulphate dialysis + ion exchange chromatography	*Streptomyces brollosae* NEAE-115	7.8	[37]
Salt precipitation + gel filtration + ion exchange chromatography	*Penicillium* sp.	1.9	[35]
Molecular exclusion chromatography + ion exchange chromatography	*Chaetomium* sp.	2.5	[38]
Gel filtration + Molecular exclusion chromatography + ion exchange chromatography	*Aspergillus fumigatus*	2.8	[39]
One-step physical adsorption onto CXs	Genetically engineered *Bacillus subtilis*	2.5	This work

Table 2 provides a comparison of the purification fold obtained with some conventional procedures typically used for ASNase purification when ASNase is produced intracellularly, as well as the respective microorganism of origin. It can be seen that the purification fold achieved in this work (2.5), through a one-step ASNase purification process, can be compared to the traditional purification techniques, and which involve three or more steps. For example, a three-step purification process for ASNase from *Penicillium* sp., involving initial salt precipitation, separation on sephadex G-100–120 gel filtration and ion exchange chromatography, revealed a purity increase of 1.9-fold [35]. This demonstrates the potential of using immobilization through physical adsorption onto CXs as a one-step purification method for ASNase, achieving similar or higher purification folds, compared to traditional purification processes, while requiring lower processing times and costs.

3.2.2. *Protein desorption from CXs*

When the purification of an enzyme is intended, the desorption process of proteins from the support material is a fundamental aspect. Since it was proved that ASNase does not adsorb on the CX material, but remains in solution in the supernatant, it was not necessary to consider the isoelectric point of the enzyme ASNase for the desorption step. The main purpose of the desorption step is to regenerate the material to be used in subsequent purifications cycles (reusability), by desorbing the unwanted proteins. Thus, extreme desorption conditions can be used as the proteins adsorbed on the material are not of interest.

The effect of pH on protein desorption was the first investigated method. The decision on the pH value to use was based on creating unfavorable conditions for undesirable proteins. For that, the CXs with adsorbed proteins were placed in contact with a citrate buffer solution pH 4. Nevertheless, after 1 h, only 14 % of the adsorbed proteins were desorbed/removed. Subsequently, protein desorption from CXs was analyzed by salt addition, i.e., the bioconjugate was placed in contact with a 5 M NaCl solution. However, an even lower removal of adsorbed

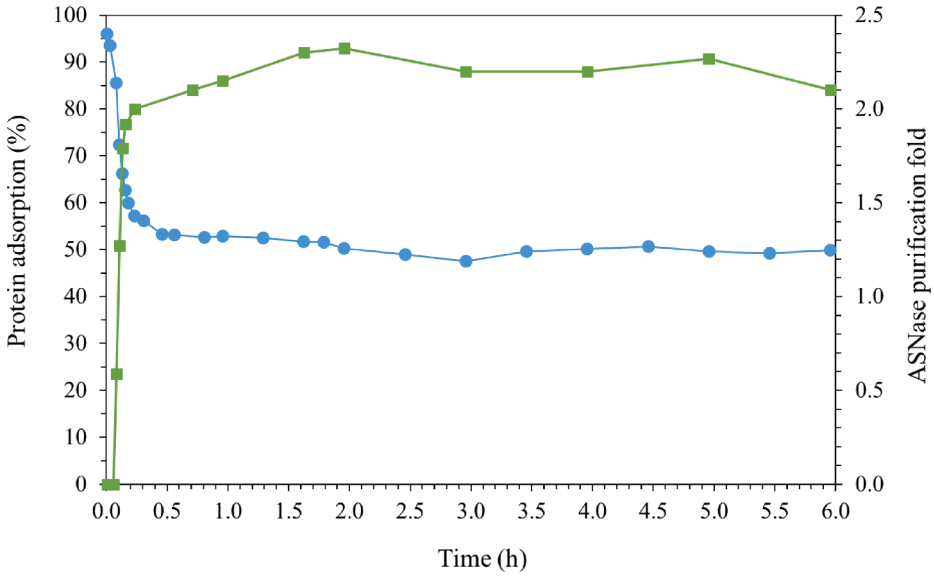

Fig. 3. Evolution of the percentage of total protein adsorbed (●) and ASNase purification fold (■) during the first test of semi-continuous ASNase purification at room temperature from a cell extract containing 3 mg/mL of total protein at flow rate of 1 mL/min using CXs.

proteins was observed, corresponding to 8 %. Other authors also reported only moderate removal of non-specific bound contaminating proteins during a salt washing using up to 2 M NaCl after the ASNase purification by immobilization onto an affinity adsorbent [40]. Finally, the effect of increasing the temperature up to 80 °C was studied, resulting in a 20 % desorption of the proteins adsorbed on the CXs. Among the tested methods, temperature showed the highest potential for protein desorption from CXs. This can be explained by the increased mobility of proteins at the interface with increasing temperatures [41].

The desorption methods used did not have the ability to completely regenerate the support material under study. Therefore, the reusability of CXs for subsequent ASNase purification processes may not be as efficient as in the initial use. However, considering the high cost of ASNase, CXs will always be of high interest for its purification, even if limited to single use applications.

3.3. Semi-continuous purification of ASNase from the cell extract

3.3.1. First ASNase purification test

After confirming that CXs are promising for the purification of ASNase from a cell extract under batch conditions, the viability of these materials to be applied in a semi-continuous purification process was analyzed. For this purpose, a glass column packed with a 5 cm height bed of previously degassed CXs was used. In the initial assay, a cell extract with a total protein concentration of 3 mg/mL and a specific ASNase activity of 0.022 U/mg was fed into the column, at a flow rate of 1 mL/min. Several samples were collected from the column outlet at various time intervals to measure the total protein concentration and ASNase activity, after contact in the column with CXs.

Fig. 3 shows that, initially, most non-target proteins present in the cell extract were adsorbed onto the packed CXs. However, as the extract flows through the purification column, a fraction of proteins started to appear in the outlet stream, resulting in a decrease in the percentage of protein adsorption onto the CXs to approximately 56 %, after 30 min of column operation. The initial high protein adsorption can be explained by the high adsorption capacity of CXs at the beginning of the assay, the amount of packed material in the column, as well as their high surface area. Subsequently, the protein adsorption started to stabilize around 50 % and remained constant until 6 h.

These results suggest that the adsorption of proteins onto CXs pores may occur in multiple layers. The initial 30 min likely corresponds to the adsorption of the first layer of proteins onto all the packed material in the column. Afterward, subsequent layers of proteins are adsorbed, indicating a constant adsorption capacity of the CXs. The variation in adsorption between the first layer and subsequent layers can be explained by the Guggenheim-Anderson-De Boer model [42], commonly used to represent multilayer protein adsorption data. This model assumes an equal state of adsorbed molecules in all layers, except for the initial layer. The results obtained are in agreement with the outcomes of the batch tests, where a protein adsorption of 45 % was obtained.

Another important parameter to evaluate is the ASNase purification fold throughout the column operation time. The ASNase activity values in the outlet stream were compared to those of the initial cell extract, revealing a purification-fold of approximately 1.8 after 1 h of contact with the packed CXs. After 2 h of operation, purification values close to those achieved in the batch process were obtained, ranging from 2.1 and 2.3 (Fig. 3). These results reveal the promising potential of using packed CXs as a one-step ASNase purification process directly from the cell extract, when compared to values reported by other authors – cf. Table 2.

Gehlot et al. [43] achieved a similar purification of 2.55-fold, related to a crude extract from *Lysinibacillus fusiformis* NP_MK, although with a two-step anion exchange chromatography purification process. Furthermore, ASNase from *Aspergillus niger*, grown in solid-state cells, was purified by Mishra [44], in a two-step process involving ammonium sulphate precipitation and DEAE cellulose column chromatography, resulting in a purification-fold of 1.44.

3.3.2. Protein desorption and CXs reusability

After the initial purification test, the desorption of proteins adsorbed onto the CXs present in the column was performed using the method that showed the most promising results in the batch tests: temperature increase. The column feed was changed to distilled water at 50 °C, with a flow rate of 1.5 mL/min, while the total protein concentration was measured at the column outlet. In the beginning of the desorption process, a protein concentration of 3.3 mg/mL was desorbed, which gradually decreased until approximately 4 h of column operation (Figure S6 in the Supporting Information). After that point, the desorption stabilized at a concentration of around 0.15 mg/mL. After 24 h, this method achieved a desorption of approximately 21 % of the total protein that was adsorbed during the first ASNase purification test. These desorption results were similar to those obtained during the protein desorption

Table 3
Total protein, total activity, ASNase specific activity, adsorption yield and purification fold of the crude and purified cell extract upon 2 purification cycles.

Cycle	Cell Extract	Total Protein (mg/mL)	Total Activity (U)	ASNase Specific Activity (U/mg)	Adsorption Yield (%)	Purification Fold
1	Crude	3	24	0.022	50	2.3
	Purified	1.5	28	0.051		
2	Crude	2.5	11	0.012	36	3.8
	Purified	1.6	26	0.046		

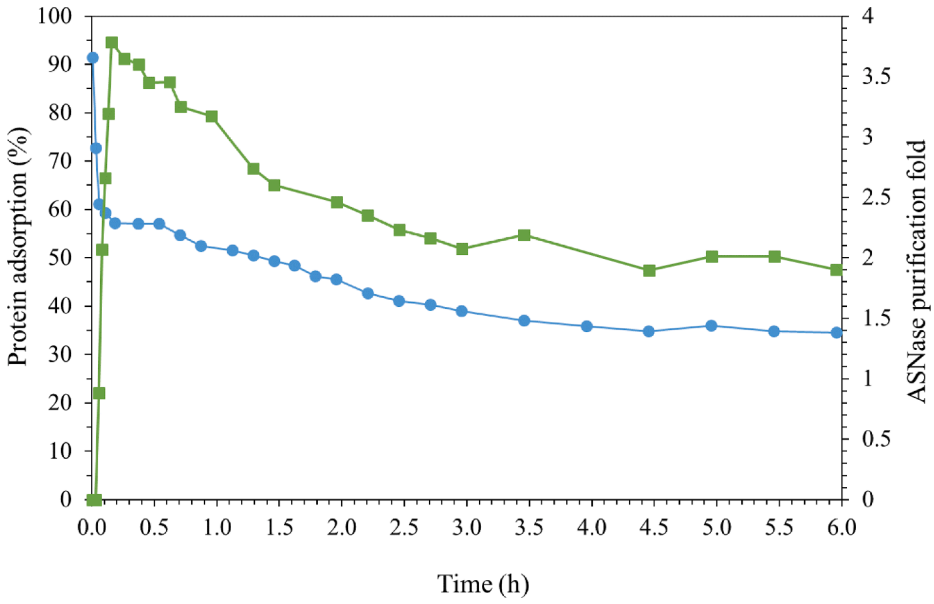

Fig. 4. Total protein adsorption (●) and ASNase purification fold (■) during the second test of semi-continuous ASNase purification at room temperature from a cell extract (2.5 mg/mL) at a flow rate of 1 mL/min using CXs.

studies in batch conditions.

After the desorption stage, in order to evaluate the reusability of the CXs purification column, a second ASNase purification test was carried out by feeding the column with a cell extract containing a total protein concentration of 2.5 mg/mL and a specific ASNase activity of 0.012 U/mg, at a flow rate of 1 mL/min (Table 3). Fig. 4 shows that, similarly to what was observed in the first purification test, during the initial minutes of operation, almost all the proteins from the cell extract were adsorbed onto CXs, reaching a protein adsorption of 57 % after 30 min of column operation. However, after that time, protein adsorption did not stabilize, but steadily decreased to a minimum of approximately 36 %, at the end of 4 h of purification column operation. From that point onwards, protein adsorption stabilized. This decrease is probably because, in this second purification test, the material already had some proteins adsorbed from the previous test. As the CXs were not totally regenerated after the first purification test, their protein adsorption capacity decreased in the second test.

In this second purification test, a maximum ASNase purification fold of 3.8 was achieved after 10 min of operation. In fact, higher purification folds were obtained during the first 2 h (Fig. 4), compared to the results obtained in the first test (Fig. 3). This difference can be attributed to the lower specific activity of ASNase in the feed stream, which was approximately 50 % lower than in the first test. These results confirm that CXs show a higher affinity for the remaining proteins in the cell extract, not adsorbing ASNase. Similarly, the percentage of adsorbed proteins and the purification fold decreased throughout the second purification test. At the end of 6 h of operation, a purification fold of approximately 2.0 was achieved. These results are in agreement with the observed increase in protein concentration verified in the outlet stream of the purification column over time, indicating reduced protein adsorption onto CXs, and consequently lowering the ASNase purification fold obtained at the column outlet.

Table 3 provides a clear summary of the results obtained for the purification of ASNase from the cell extract upon the first and second cycles of adsorption. The use of immobilization by physical adsorption onto CXs as a one-step ASNase purification process from a cell extract of *B. subtilis* shows great potential, by achieving purification folds currently only possible using multi-step processes and high-cost chromatographic techniques. In order to reach the high relative activity values required for industrial applications, a post-concentration step would be necessary.

4. Conclusions

CXs materials were here investigated, for the first time, aiming to develop a one-step platform, operating by the flow-through-like mode, for the purification of ASNase from cell extracts. After CXs synthesis and characterization ($r_p = 6.3$ nm; $V_p = 0.80$ cm^3/g; S_{BET}=688 m^2/g; average particle size = 252 μm), batch tests were first performed to optimize three experimental parameters (cell extract concentration, CXs amount and adsorption volume) to maximize the ASNase purification fold. In these batch adsorption tests, a ASNase purification fold of 2.5 was achieved by adsorbing a 3 mg/mL of cell extract onto 18 mg of CXs in 15 mL flasks. This purification fold, combined with the results of SDS-PAGE analysis, showed that CXs were able to selectively isolate the target enzyme (ASNase) in the supernatant, while adsorbing the remaining and undesired proteins. Although the tested protein desorption methods (pH change, NaCl addition, temperature increase) were unable to completely regenerate the CXs, yielding only around 20 % of protein desorption, the semi-continuous purification experiments performed with the synthesized CXs packed in a column resulted in an ASNase purification fold of 3.8 in a second purification test. This value is similar to or higher than

those reported in the literature and achieved with multi-step and expensive chromatographic techniques.

The obtained results reveal that the one-step ASNase purification from a cell extract using CXs is a simple, fast, and cost-effective method, representing a promising platform for the pharmaceutical and food industries, and which may serve as a pre-purification step prior to the final polishing stage. This method significantly reduces the concentration of the other proteins in the cell extract, thus effectively minimizing the required number of purification processing steps and the associated downstream costs.

CRediT authorship contribution statement

Raquel O. Cristóvão: Investigation, Methodology, Validation, Writing – original draft. **Rita A.M. Barros:** Investigation, Methodology, Validation. **Teresa P. Marramaque:** Investigation, Methodology, Validation. **Gonçalo G. Aguiar:** Investigation, Methodology, Validation. **Mafalda R. Almeida:** Investigation, Methodology, Validation. **Sónia A. C. Carabineiro:** Investigation, Methodology, Resources, Funding acquisition, Writing – review & editing. **Gabriela B. de Paiva:** Investigation, Methodology, Validation. **Danielle B. Pedrolli:** Investigation, Methodology, Validation. **Mara G. Freire:** Investigation, Methodology, Resources, Funding acquisition, Writing – review & editing. **Joaquim L. Faria:** Investigation, Methodology, Resources, Funding acquisition, Writing – review & editing. **Valéria C. Santos-Ebinuma:** Investigation, Methodology, Resources, Funding acquisition, Writing – review & editing. **Ana P.M. Tavares:** Investigation, Methodology, Resources, Funding acquisition, Writing – review & editing, Supervision. **Cláudia G. Silva:** Investigation, Methodology, Resources, Funding acquisition, Writing – review & editing, Supervision.

Declaration of competing interest

The authors declare that they have no known competing financial interests or personal relationships that could have appeared to influence the work reported in this paper.

Data availability

No data was used for the research described in the article.

Acknowledgments

This work was supported by national funds through FCT/MCTES (PIDDAC): LSRE-LCM, UIDB/50020/2020 (DOI: 10.54499/UIDB/50020/2020) and UIDP/50020/2020 (DOI: 10.54499/UIDP/50020/2020); and ALiCE, LA/P/0045/2020 (DOI: 10.54499/LA/P/0045/2020). It was also supported by POCI-01-0145-FEDER-031268 funded by FEDER, through COMPETE2020-Programa Operacional Competitividade e Internacionalização (POCI), and by national funds (OE), through FCT/MCTES. This work was developed partly within the scope of the project CICECO-Aveiro Institute of Materials, UIDB/50011/2020 (DOI10.54499/UIDB/50011/2020), UIDP/50011/2020 (DOI 10.54499/UIDP/50011/2020) & LA/P/0006/2020 (DOI 10.54499/LA/P/0006/2020), financed by national funds through the FCT/MCTES (PIDDAC). This work was also partially supported by the Associate Laboratory for Green Chemistry—LAQV, financed by national funds from FCT/MCTES (DOIs: 10.54499/LA/P/0008/2020, 10.54499/UIDP/50006/2020, 10.54499/UIDB/50006/2020). Valéria C. Santos-Ebinuma and Gabriela B. de Paiva acknowledges FAPESP (Grant no. 2018/06908-8, 2021/01284-9, 2021/06686-8). Ana P.M. Tavares and Sónia A.C. Carabineiro acknowledge FCT for the research contracts CEEC-IND/2020/01867 (doi: 10.54499/2020.01867.CEECIND/CP1589/CT0013) and CEECINST/00102/2018 (DOI: 10.54499/CEECINST/00102/2018/CP1567/CT0026), respectively. R.A.M. Barros acknowledges FCT for her PhD grant 2022.12055.BD. Valeria C. Santos-Ebinuma thanks the National Council of Scientific and Technological Development, Brazil (Conselho Nacional de Desenvolvimento Científico e Tecnológico — CNPq) — grant no. 312463/2021-9. Danielle B. Pedrolli acknowledges CNPq grant 305324/2023.

Appendix A. Supplementary data

Supplementary data to this article can be found online at https://doi.org/10.1016/j.seppur.2024.128969.

References

[1] A. Ulu, B. Ates, Immobilization of l-asparaginase on carrier materials: a comprehensive review, Bioconjug. Chem. 28 (2017) 1598–1610.
[2] M.V. Pokrovskaya, V.S. Pokrovsky, S.S. Aleksandrova, N.N. Sokolov, D.D. Zhdanov, Molecular analysis of L-asparaginases for clarification of the mechanism of action and optimization of pharmacological functions, Pharmaceutics 14 (2022).
[3] D. Castro, A.S.C. Marques, M.R. Almeida, G.B. de Paiva, H.B.S. Bento, D.B. Pedrolli, M.G. Freire, A.P.M. Tavares, V.C. Santos-Ebinuma, L-asparaginase production review: bioprocess design and biochemical characteristics, Appl. Microbiol. Biotechnol. 105 (2021) 4515–4534.
[4] J.F. Buyel, R. Fischer, Downstream processing of biopharmaceutical proteins produced in plants: the pros and cons of flocculants, Bioengineered 5 (2014) 138–142.
[5] A. Ramakrishnan, A. Sadana, in: Economics of Bioseparation Processes, Separation Science and Technology, Academic Press, 2000, pp. 667–685.
[6] Y.D. Clonis, N.E. Labrou, V.P. Kotsira, C. Mazitsos, S. Melissis, G. Gogolas, Biomimetic dyes as affinity chromatography tools in enzyme purification, J. Chromatogr. A 891 (2000) 33–44.
[7] X. Zeng, E. Ruckenstein, Membrane chromatography: preparation and applications to protein separation, Biotechnol. Prog. 15 (1999) 1003–1019.
[8] A.S. Rathore, D. Kumar, N. Kateja, Recent developments in chromatographic purification of biopharmaceuticals, Biotechnol. Lett 40 (2018) 895–905.
[9] M. Shanmugaprakash, C. Jayashree, V. Vinothkumar, S.N.S. Senthilkumar, S. Siddiqui, V. Rawat, M. Arshad, Biochemical characterization and antitumor activity of three phase partitioned l-asparaginase from Capsicum annuum L, Sep. Purif. Technol. 142 (2015) 258–267.
[10] E.A. Makky, Y. Chun Loh, M.R. Karim, Purification and partial characterization of a low molecular weight l-asparaginase produced from corn cob waste, Biocatal. Agric. Biotechnol. 3 (2014) 265–270.
[11] A. Badoei-Dalfard, Purification and characterization of l-asparaginase from Pseudomonas aeruginosa strain SN004: Production optimization by statistical methods, Biocatal. Agric. Biotechnol. 4 (2015) 388–397.
[12] A. Khushoo, Y. Pal, B.N. Singh, K.J. Mukherjee, Extracellular expression and single step purification of recombinant Escherichia coli L-asparaginase II, Protein Expr. Purif. 38 (2004) 29–36.
[13] S. Yim, M. Kim, Purification and characterization of thermostable l-asparaginase from Bacillus amyloliquefaciens MKSE in Korean soybean paste, LWT 109 (2019) 415–421.
[14] F.F.G. Dias, A.L.T.G. Ruiz, A.D. Torre, H.H. Sato, Purification, characterization and antiproliferative activity of l-asparaginase from Aspergillus oryzae CCT 3940 with no glutaminase activity, Asian Pac. J. Trop. Biomed. 6 (2016) 785–794.
[15] J. Bhagat, A. Kaur, B.S. Chadha, Single step purification of asparaginase from endophytic bacteria Pseudomonas oryzihabitans exhibiting high potential to reduce acrylamide in processed potato chips, Food Bioprod. Process. 99 (2016) 222–230.
[16] N.S. Mohan Kumar, H.K. Manonmani, Purification, characterization and kinetic properties of extracellular L-asparaginase produced by Cladosporium sp, World J. Microbiol. Biotechnol. 29 (2013) 577–587.
[17] A.M. Azevedo, P.A. Rosa, I.F. Ferreira, M.R. Aires-Barros, Integrated process for the purification of antibodies combining aqueous two-phase extraction, hydrophobic interaction chromatography and size-exclusion chromatography, J. Chromatogr. A 1213 (2008) 154–161.
[18] S. Dutta, S. Ghosh, S. Pramanik, L-asparaginase and L-glutaminase from Aspergillus fumigatus WL002: Production and some physicochemical properties, Appl. Biochem. Microbiol. 51 (2015) 425–431.
[19] L. Facchinetti de Castro Girão, S.L. Gonçalves da Rocha, R.S. Sobral, A.P. Dinis Ano Bom, A.L. Franco Sampaio, J. Godinho da Silva, Jr., M.A. Ferrara, E. Pinto da Silva Bon, J. Perales, Saccharomyces cerevisiae asparaginase II, a potential antileukemic drug: Purification and characterization of the enzyme expressed in Pichia pastoris, Protein expression and purification, 120 (2016) 118-125.
[20] J.C.F. Nunes, M.R. Almeida, G.B. de Paiva, D.B. Pedrolli, V.C. Santos-Ebinuma, M. C. Neves, M.G. Freire, A.P.M. Tavares, A flow-through strategy using supported ionic liquids for L-asparaginase purification, Sep. Purif. Technol. 315 (2023) 123718.
[21] R.O. Cristóvão, M.R. Almeida, M.A. Barros, J.C.F. Nunes, R.A.R. Boaventura, J. M. Loureiro, J.L. Faria, M.C. Neves, M.G. Freire, V.C. Ebinuma-Santos, A.P. M. Tavares, C.G. Silva, Development and characterization of a novel l-asparaginase/MWCNT nanobioconjugate, RSC Adv. 10 (2020) 31205–31213.
[22] R.O. Cristóvão, R.A.M. Barros, J.G. Pinho, L.S. Teixeira, M.C. Neves, M.G. Freire, J. L. Faria, V.C. Santos-Ebinuma, A.P.M. Tavares, C.G. Silva, Unveiling the Influence

of Carbon Nanotube Diameter and Surface Modification on the Anchorage of L-Asparaginase, Appl. Sci. (2022).
[23] R.A.M. Barros, R.O. Cristóvão, S.A.C. Carabineiro, M.C. Neves, M.G. Freire, J.L. Faria, V.C. Santos-Ebinuma, A.P.M. Tavares, C.G. Silva, Immobilization and Characterization of L-Asparaginase over Carbon Xerogels, Biotech (Basel (Switzerland)), 11 (2022).
[24] R.A.M. Barros, R.O. Cristóvão, I.G. Carneiro, M.A. Barros, M.M. Pereira, S.A. C. Carabineiro, M.G. Freire, J.L. Faria, V.C. Santos-Ebinuma, A.P.M. Tavares, C. G. Silva, Improved L-asparaginase properties and reusability by immobilization onto functionalized carbon xerogels, ChemPlusChem (2024) e202400025.
[25] S.J. Segovia-Sandoval, L.M. Pastrana-Martínez, R. Ocampo-Pérez, S. Morales-Torres, M.S. Berber-Mendoza, F. Carrasco-Marín, Synthesis and characterization of carbon xerogel/graphene hybrids as adsorbents for metronidazole pharmaceutical removal: effect of operating parameters, Sep. Purif. Technol. 237 (2020) 116341.
[26] H.B.S. Bento, G.B. Paiva, M.R. Almeida, C.G. Silva, P.J. Carvalho, A.P.M. Tavares, D.B. Pedrolli, V.C. Santos-Ebinuma, Aliivibrio fischeri L-Asparaginase production by engineered Bacillus subtilis: a potential new biopharmaceutical, Bioprocess Biosyst. Eng. 45 (2022) 1635–1644.
[27] S. Kumar, Isolation and Purification of High Efficiency L-asparaginase by Quantitative Preparative Continuous-elution SDS, PAGE Electrophoresis, 2011.
[28] P.V. Samant, F. Gonçalves, M.M.A. Freitas, M.F.R. Pereira, J.L. Figueiredo, Surface activation of a polymer based carbon, Carbon 42 (2004) 1321–1325.
[29] N. Mahata, M.F.R. Pereira, F. Suárez-García, A. Martínez-Alonso, J.M.D. Tascón, J. L. Figueiredo, Tuning of texture and surface chemistry of carbon xerogels, J. Colloid Interface Sci. 324 (2008) 150–155.
[30] M.H. Simonian, J.A. Smith, Spectrophotometric and Colorimetric Determination of Protein Concentration, 10 (2001) A.3G.1-A.3G.9.
[31] A. Jorio, A.G. Souza Filho, Raman studies of carbon nanostructures, Annu. Rev. Mat. Res. 46 (2016) 357–382.
[32] A.C. Ferrari, J. Robertson, Interpretation of Raman spectra of disordered and amorphous carbon, Phys. Rev. B 61 (2000) 14095–14107.
[33] M. Kozak, S. Jurga, A comparison between the crystal and solution structures of Escherichia coli asparaginase II, Acta Biochim. Pol. 49 (2002) 509–513.
[34] H.P. Erickson, Size and shape of protein molecules at the nanometer level determined by sedimentation, gel filtration, and electron microscopy, Biological Procedures Online 11 (2009) 32–51.
[35] K.K.R. Patro, N. Gupta, Extraction, purification and characterization of L-asparaginase from Penicillium sp, By Submerged Fermentation (2012).
[36] N.-E.-A. El-Naggar, S.F. Deraz, H.M. Soliman, N.M. El-Deeb, S.M. El-Ewasy, Purification, characterization, cytotoxicity and anticancer activities of L-asparaginase, anti-colon cancer protein, from the newly isolated alkaliphilic Streptomyces fradiae NEAE-82, Sci. Rep. 6 (2016) 32926.
[37] N.-E.-A. El-Naggar, S.F. Deraz, S.M. El-Ewasy, G.M. Suddek, Purification, characterization and immunogenicity assessment of glutaminase free L-asparaginase from Streptomyces brollosae NEAE-115, BMC Pharmacol. Toxicol. 19 (2018) 51.
[38] N. Arumugam, P. Thangavelu, Purification and anticancer activity of glutaminase and urease free intracellular l-asparaginase from Chaetomium sp, Protein Expr. Purif. 190 (2022) 106006.
[39] M.A. Yassin, A. Shindia, M. Labib, M. Soud, A.S.A. El-Sayed, Thermostable Chitosan-L-Asparaginase conjugate from Aspergillus fumigatus is a novel structurally stable composite for abolishing acrylamide formation in French fried potatoes, LWT 162 (2022) 113494.
[40] C.S. Karamitros, N.E. Labrou, Extracellular expression and affinity purification of L-asparaginase from E. chrysanthemi in E. coli, Sustainable Chemical Processes, 2 (2014) 16.
[41] I. Kiesel, M. Paulus, J. Nase, S. Tiemeyer, C. Sternemann, K. Rüster, F.J. Wirkert, K. Mende, T. Büning, M. Tolan, Temperature-driven adsorption and desorption of proteins at solid-liquid interfaces, Langmuir 30 (2014) 2077–2083.
[42] E.O. Timmermann, A.B.E.T.-like three sorption stage isotherm, Journal of the Chemical Society, Faraday Transactions 1: Physical Chemistry in Condensed Phases, 85 (1989) 1631-1645.
[43] P. Gehlot, M. Kumar, N. Pareek, Production and purification of glutaminase free L-asparaginase from Lysinibacillus fusiformis and its appraisal in acrylamide mitigation of starchy foods, Materials Today: Proceedings, 69 (2022) 64-73.
[44] A. Mishra, Production of l-asparaginase, an anticancer agent, from Aspergillus niger using agricultural waste in solid state fermentation, Appl. Biochem. Biotechnol. 135 (2006) 33–42.